

## Supplementary Information

# On-surface synthesis of organometallic nanorings linked by unconventional intermediates of Ullmann reaction

Xiaoyang Zhao<sup>†a</sup>, Liqian Liu<sup>†a</sup>, Zhipeng Zhang<sup>a</sup>, Tianchen Qin<sup>b</sup>, Jun Hu<sup>b</sup>, Lei Ying<sup>a</sup>, Junfa Zhu<sup>b</sup>, Tao Wang<sup>c\*</sup>, Xinrui Miao<sup>a\*</sup>

<sup>a</sup>Institute of Polymer Optoelectronic Materials and Devices, State Key Laboratory of Luminescent Materials and Devices, College of Materials Science and Engineering, South China University of Technology, Guangzhou 510640, P. R. China

<sup>b</sup>National Synchrotron Radiation Laboratory, University of Science and Technology of China, Hefei, 230029, P. R. China

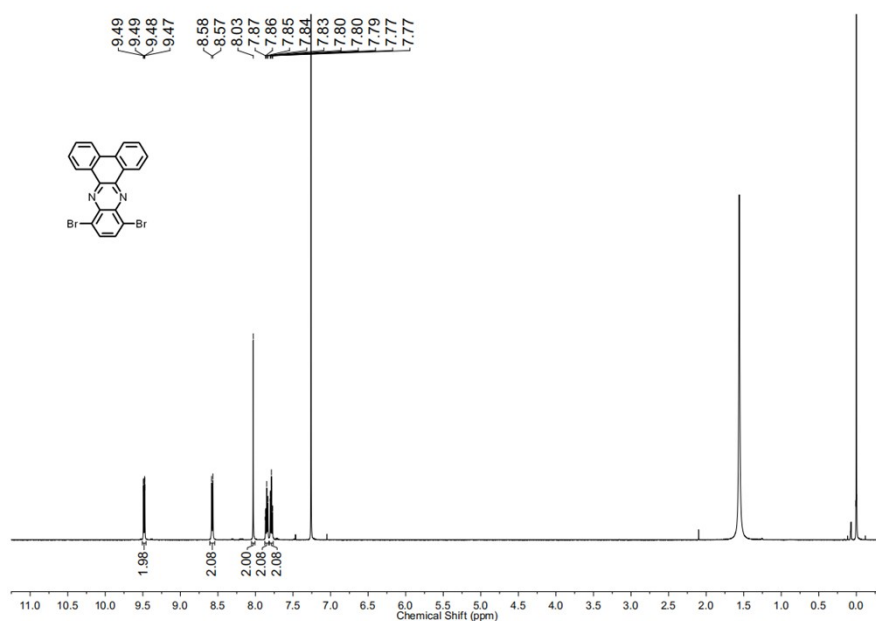
<sup>c</sup>State Key Laboratory of Organometallic Chemistry, Shanghai Institute of Organic Chemistry, Chinese Academy of Sciences, Shanghai, 200032, P. R. China

**Corresponding authors:** Xinrui Miao (msxrmiao@scut.edu.cn)  
Tao Wang (taowang@sioc.ac.cn)

<sup>†</sup> These authors contributed equally.

## Methods

**Sample preparation.** 10,13-Dibromodibenzo[*a,c*]phenazine (DBP-Br) molecule was provided by Ying's group (purity higher than 98%).  $^1\text{H}$  NMR (298 K, 400 MHz,  $\text{CDCl}_3$ )  $\delta$  9.49 (d, 2H), 8.57 (d, 2H), 8.03 (s, 2H), 7.83 – 7.87 (m, 2H), 7.77 – 7.80 (m, 2H). The single crystalline Cu(111) surface was cleaned through cycles of  $\text{Ar}^+$  ion sputtering (1.5 keV) and followed by annealing at 750 K for 20 min. DBP-Br molecules were then deposited onto the clean Cu(111) surface maintained at room temperature using a molecular evaporator heated to 403 K, with the deposition time of 10, 5, and 2 mins to obtain the different molecular coverages. The sample was annealed for 20 mins at each elevated temperature shown in main text.



$^1\text{H}$  NMR spectrum of DBP-Br

**STM/AFM characterization.** All STM images were obtained using a low-temperature STM (Scienta Omicron), maintaining a typical base pressure below  $2 \times 10^{-10}$  mbar at 77 K. nc-AFM experiments were carried out in constant-height frequency modulation mode using a combined STM/AFM system (CreaTec) at 4.7 K with a base pressure below  $5 \times 10^{-10}$  mbar. The qPlus sensor was equipped with a CO-functionalized tungsten tip (sensor stiffness  $k_0 \approx 1800$  N/m, resonance frequency  $f_0 = 29$  kHz, and the quality factor  $Q \approx 14000$ ). STM images were captured in constant-current mode. The data were processed using WSxM software.<sup>1</sup>

**Synchrotron radiation photoemission spectroscopy (SRPES).** The SRPES measurements were carried out at the Catalysis and Surface Science Endstation of the National Synchrotron Radiation Laboratory, Hefei, China. Sample preparation was carried out in the same way as described for the STM measurements.<sup>2</sup> SRPE spectra were acquired at an emission angle of  $50^\circ$  with respect to the surface normal. The C 1s, N 1s and Br 3d spectra were collected with photon energies of 380, 500 and

220 eV, respectively. The chosen emission angle and photon energy aimed to render the XPS surface-sensitive. All SRPES data are fitted by Avantage software, version 5.9922 from Avantage Software Ltd (United Kingdom). The SRPES spectra obtained from samples with the same element annealed at different temperatures are fitted with uniform fitting parameters to ensure the reliability and accuracy of results. Specifically, the full width at half maximum (FWHM) is restricted to 0.5–1 eV, the Lorentz: Gaussian mixing (L/G Mix) is fixed at 30%: 70%, the tail mixing value is 100%, and the tail height and tail exponent are 0%. Peak assignments for different chemical species are subsequently performed using the automatic fitting implemented in the Avantage software package.

**Theoretical calculation.** Density functional theory (DFT) calculations were conducted using the Vienna ab Initio Simulation Package (VASP).<sup>3, 4</sup> The projector-augmented wave method was employed to describe the interaction between ions and electrons.<sup>5, 6</sup> The generalized gradient approximation (GGA) with Perdew–Burke–Ernzerhof (PBE) formalism was utilized to depict the exchange–correlation interaction,<sup>7</sup> and van der Waals interactions were accounted for using the DFT-D3 method developed by Grimme.<sup>8</sup> The atomic structures were relaxed until the forces on all unconstrained atoms were  $\leq 0.05$  eV/Å. In order to balance the feasibility and accuracy of calculation results, some systems were simulated by one or two-layered Cu(111) slabs separated by at least 20 Å for the charge density difference, electron localization function, and energy calculations. This approach effectively analyzes systems without requiring the excessive resources for more complex multi-layered models, ensuring the reliability of the findings within practical limits. The wave functions were expanded using planewave basis sets with a cutoff energy of 450 eV. STM images were simulated employing the Tersoff-Hamann approximation with the implementation by Lorente and Persson.<sup>9</sup> The transition states (TS) were determined using the VTST code with the climbing image nudged elastic band (CI-NEB) method.<sup>10, 11</sup> The initial states (IS) and final states (FS) were initially fully relaxed, and 7 images were inserted between the IS and FS. The Cu(111) surface was modeled by three-layered slabs separated by at least 20 Å of vacuum and completely relaxed during the transition state search process. The structure of local minima and the saddle points were optimized until the average atomic force was lower than 0.02 eV/Å.

Partial charges of the molecules were evaluated using Bader charge analysis based on DFT-calculated electronic density. The charge density difference was evaluated by using the following equation:

$$\Delta\rho = \rho_{\text{tot}} - \rho_{\text{substrate}} - \rho_{\text{adsorbate}}$$

Where  $\rho_{\text{tot}}$  is the total charge density of the whole system, and  $\rho_{\text{substrate}}$  and  $\rho_{\text{adsorbate}}$  are the charge density of the Cu(111) substrate and the adsorbate, respectively. The quantitative charge transfer between adsorbate and Cu(111) substrate was calculated using the Bader method, employing Bader’s atom in molecule method to partition the total electron density into non-overlapping atomic volumes.

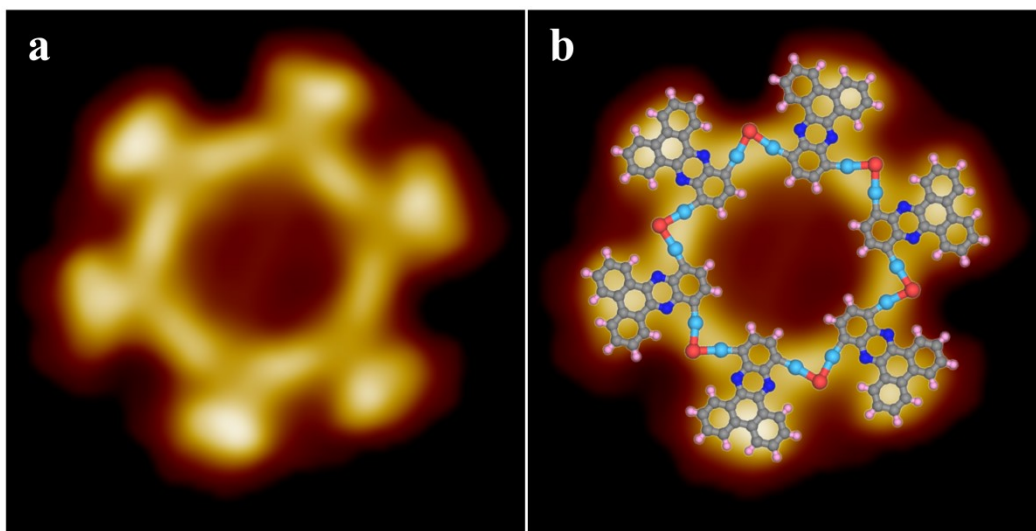


**Figure S1.** (a) Zoom-in STM image of a 6-membered ring bonded by C-Cu-Br-Cu-C. The corresponding chemical structure is overlapped in (b).

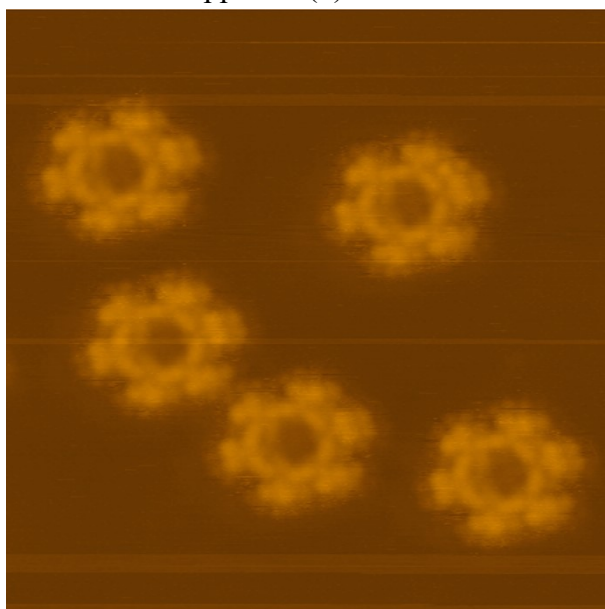


**Figure S2.** A representative STM image showing that C-Cu-Br-Cu-C linked six-membered nanorings are surrounded by Br adatoms which exhibit as small dots. These Br adatoms should be from the dissociation of C-Br bonds but did not participate in the formation of C-Cu-Br-Cu-C motifs.

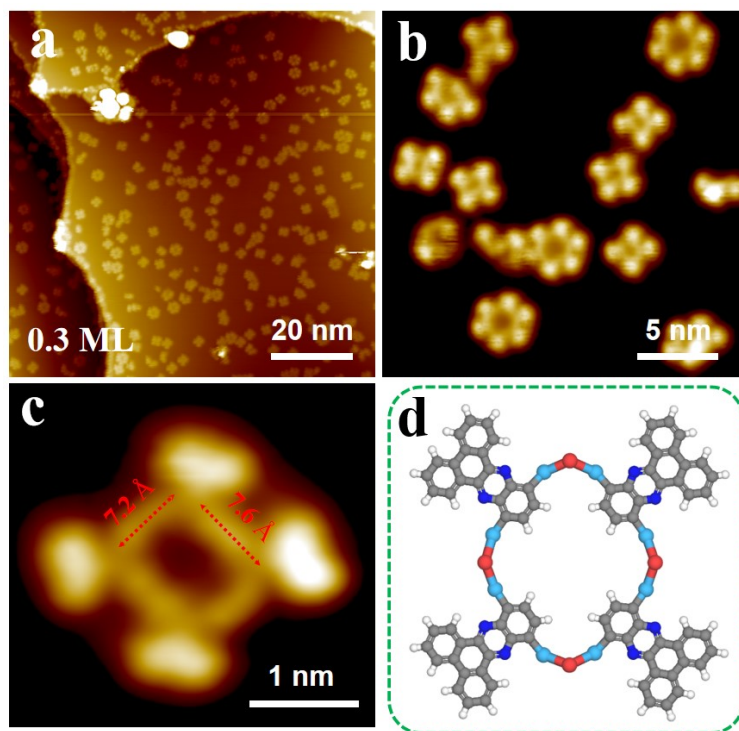


**Figure S3.** (a) Large-scale STM image recorded after depositing DBP-Br on Cu(111) held at 300 K with a coverage of  $\sim 0.3$  ML. (b) Small-scale STM image containing many 4-membered nanorings containing C–Cu–Br–Cu–C bond. (c,d) High-resolution STM image and DFT-optimized molecular model. Scanning parameters: (a-c)  $V_{\text{bias}} = 500$  mV,  $I_{\text{set}} = 50$  pA.

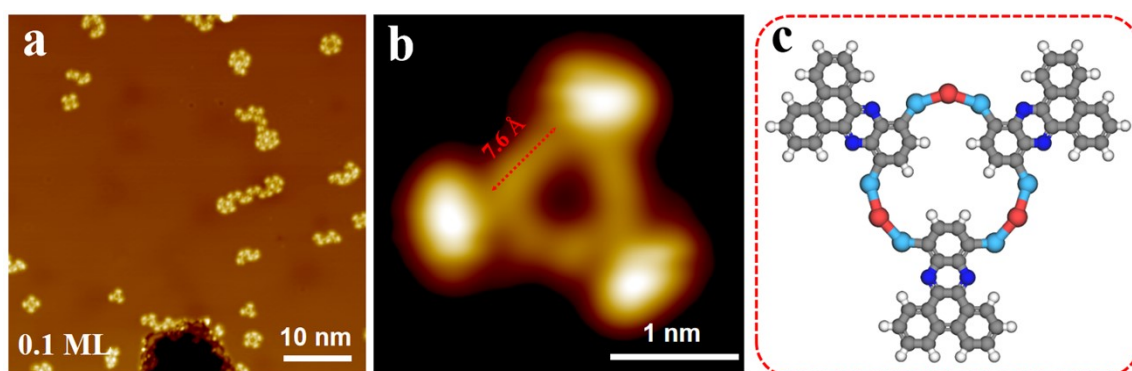


**Figure S4.** (a) STM image recorded after depositing DBP-Br molecules on Cu(111) held at 300 K with a coverage of  $\sim 0.1$  ML. The image showing the emergence of 3-membered nanorings. (b) High-resolution STM image of a 3-membered ring. (c) DFT-optimized molecular model. Scanning parameters:  $V_{\text{bias}} = 1000$  mV,  $I_{\text{set}} = 200$  pA.

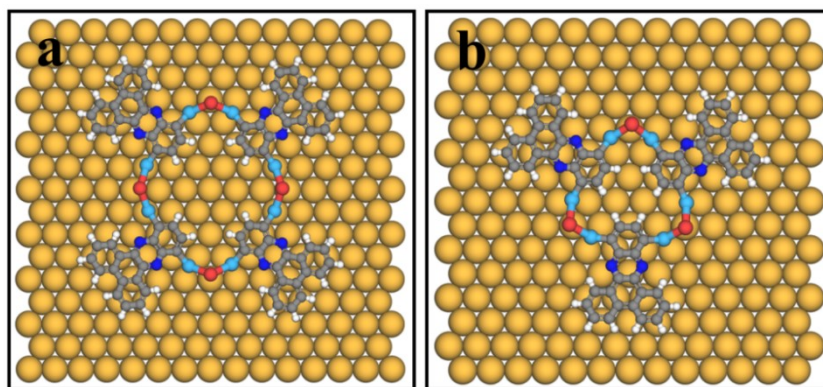


**Figure S5.** DFT-optimized molecular models of nanorings on a Cu(111) surface. (a) 4-membered nanoring. (b) 3-membered nanoring.

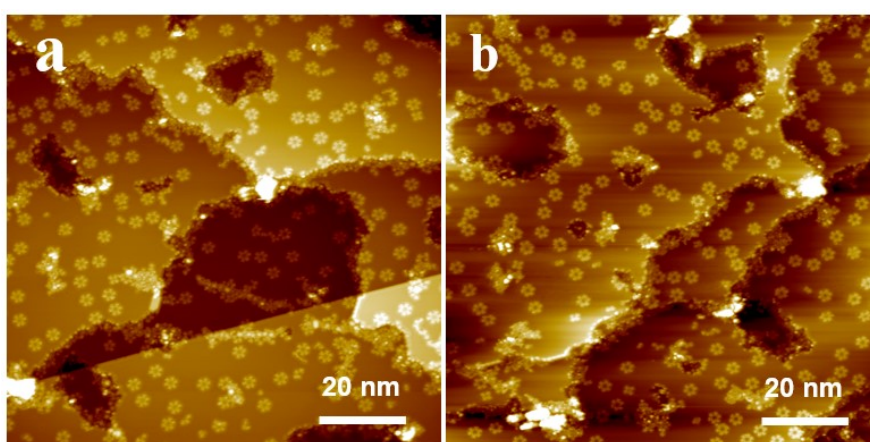


**Figure S6.** STM images of 6-membered nanorings linked through C–Cu–Br–Cu–C bonds after leaving the sample at RT for 4 days. Scanning parameters:  $V_{\text{bias}} = 500$  mV,  $I_{\text{set}} = 50$  pA. The 6-membered nanorings kept stable.

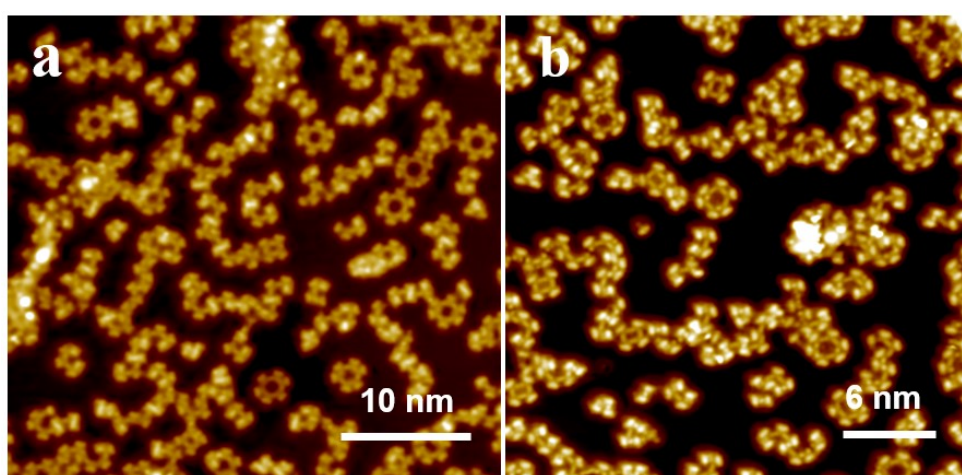


**Figure S7.** Representative STM images showing most of the 6-membered nanorings opened after annealing the sample at 333 K. Scanning parameters:  $V_{\text{bias}} = 500$  mV,  $I_{\text{set}} = 50$  pA.

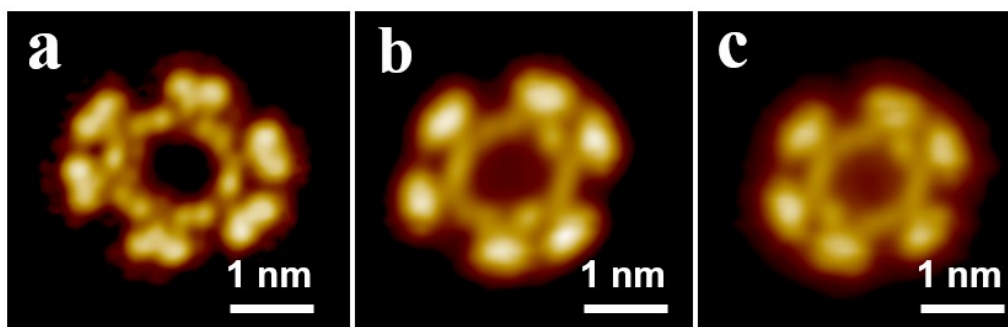


**Figure S8.** Zoom-in STM images of 6-membered nanorings with different numbers and positions of C–Cu–C bonds, containing one C–Cu–C bonds (a), two *ortho*-C–Cu–C bonds (b), and two *para*-C–Cu–C bonds (c). Scanning parameters:  $V_{\text{bias}} = 1000$  mV,  $I_{\text{set}} = 200$  pA.

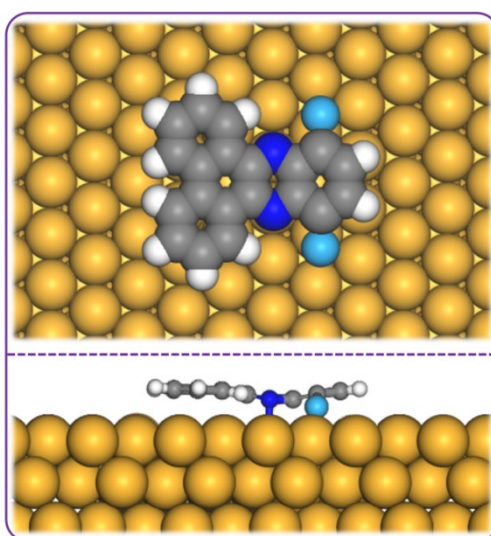


**Figure S9.** Top and side views of the conformation of a Cu–DBP–Cu species on Cu(111) displaying the formation of N–Cu coordination bond, associated with the nonplanar adsorption geometry.

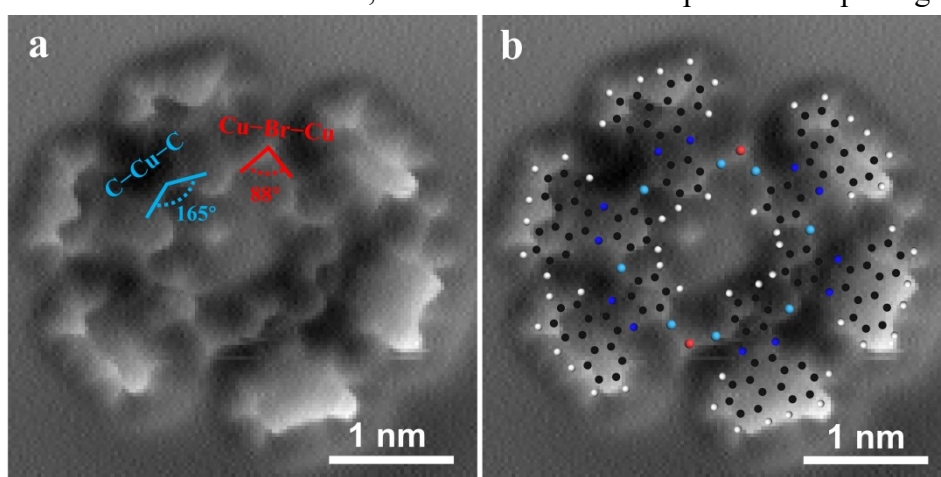


**Figure S10.** The nc-AFM images of 6-membered nanorings containing C–Cu–C and C–Cu–Br–Cu–C bonds. (a) C–Cu–C bond angle is measured as  $165^\circ$ , and the Cu–Br–Cu bond angle is measured as  $88^\circ$  in the 6-membered nanoring. (b) The corresponding nc-AFM image overlapped by chemical structure.

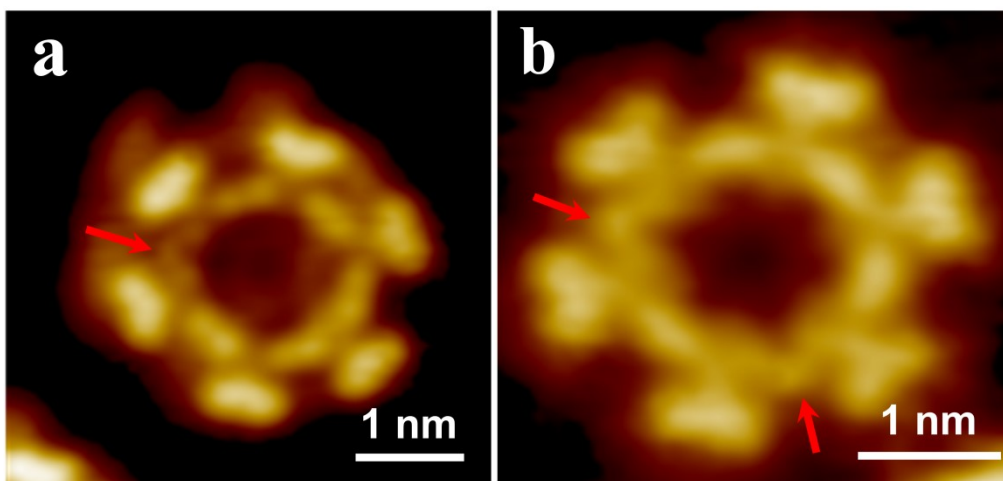


**Figure S11.** STM images displaying intermediate state for the transition from C–Cu–Br–Cu–C to C–Cu–C bond, where Br atoms move further away from the ring, as pointed out by red arrows. Scanning parameters: (a)  $V_{\text{bias}} = 1000$  mV,  $I_{\text{set}} = 200$  pA. (b)  $V_{\text{bias}} = 500$  mV,  $I_{\text{set}} = 50$  pA.

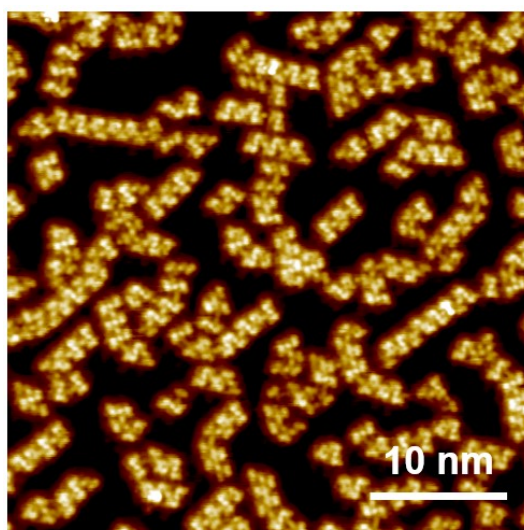


**Figure S12.** STM image displaying homogenous chain structures bonded by C–Cu–C, formed after annealing the sample at 353 K. Scanning parameters:  $V_{\text{bias}} = 500$  mV,  $I_{\text{set}} = 50$  pA.

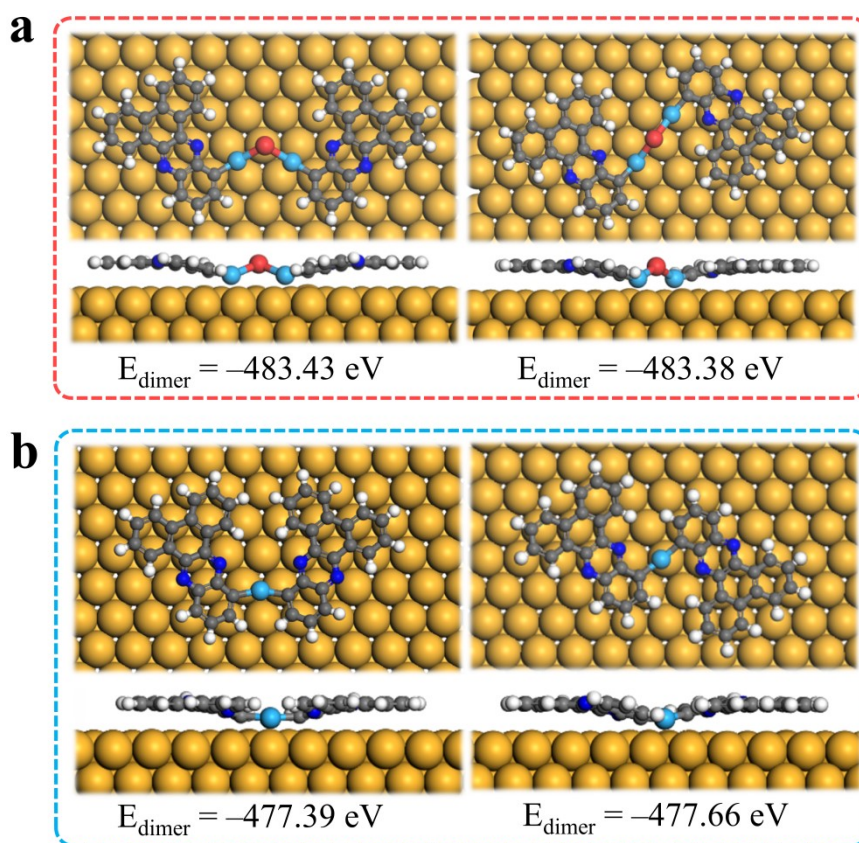


**Figure S13.** (a) DFT calculated dimer energy reveals that the C–Cu–Br–Cu–C bond is energetically more favorable for the formation of *cis*-dimer. (b) DFT calculated dimer energy reveals that the C–Cu–C bond is energetically more favorable for the formation of *trans*-dimer.

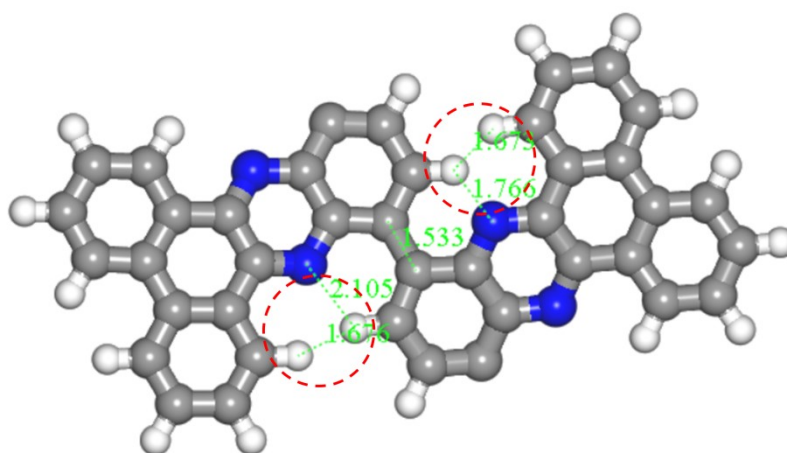


**Figure S14.** The strong steric hindrance between N and adjacent H atoms, neighboring H atoms for the formation of the covalent dimer, as indicated by dashed circles. All the distances as marked are near to the length of a covalent bond, indicating the difficulty for the formation of the C–C bond.

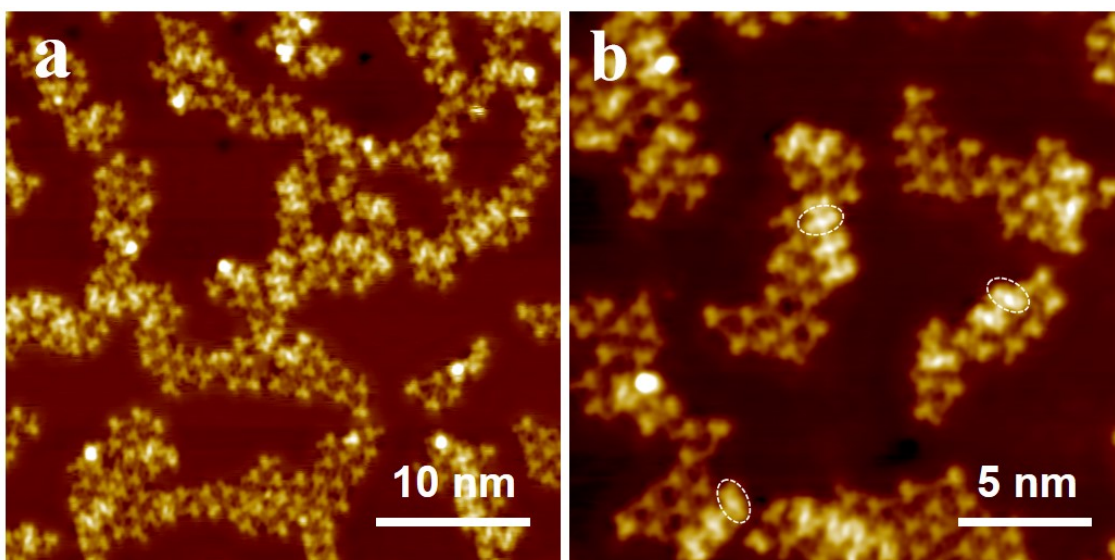


**Figure S15.** (a) Large-scale STM image and (b) enlarged STM image showing the monomer islands formed through Br $\cdots$ H bonding after annealing the sample at 413 K, where Br atoms adsorbed on Cu(111) after complete dissociations of C–Br and C–Cu–Br–Cu–C bonds. Because of the large steric hindrance as presented in Figure S14, a few covalent products were observed (marked with white dotted circles). Scanning parameters:  $V_{\text{bias}} = -600$  mV,  $I_{\text{set}} = -200$  pA.

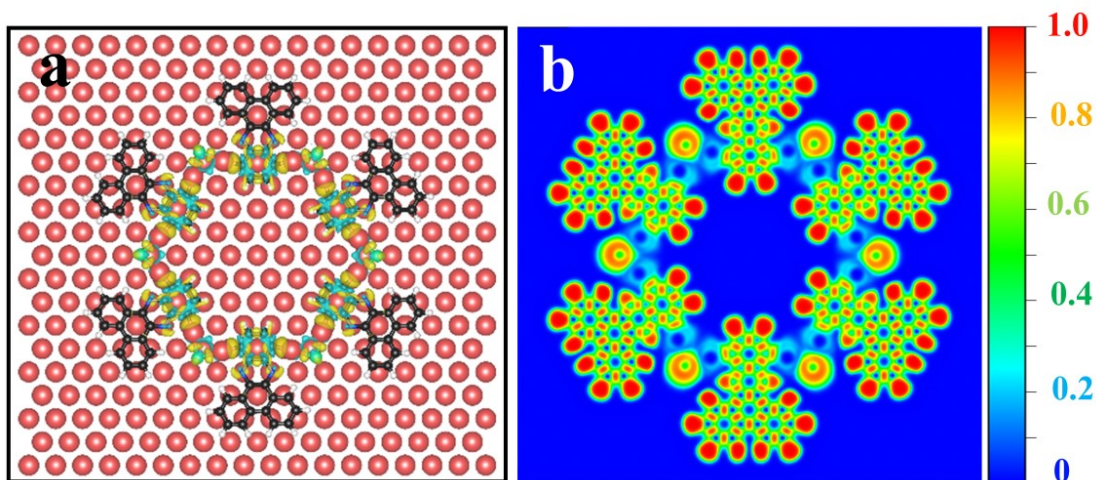


**Figure S16.** (a) Top view of charge difference plots for 6-membered nanoring with an isosurface value  $0.0025 \text{ e} \cdot \text{\AA}^{-3}$ . (b) ELF mapping of 6-membered nanoring. The isosurface value is  $0.003 \text{ e} \cdot \text{\AA}^{-3}$ .

The charge density difference plot reveals the evident electron donation from coordinated Cu adatoms ( $\text{Cu}_{\text{ad}}$ ) to bonded C atoms ( $\text{C}_{\text{b}}$ ) and bonded Br atoms ( $\text{Br}_{\text{b}}$ ) in the 6-membered nanoring (Figure S16a). Bader charge analysis shows that the amount of charge transferred from  $\text{Cu}_{\text{ad}}$  to  $\text{C}_{\text{b}}$  atom and  $\text{Cu}_{\text{ad}}$  to  $\text{Br}_{\text{b}}$  atom are  $0.19 \text{ e}$  and  $0.47 \text{ e}$ , respectively. From these calculation results, 28.7% of the electrons transferred from  $\text{Cu}_{\text{ad}}$  to  $\text{C}_{\text{b}}$  atom, and 71.3% of the electrons transferred from  $\text{Cu}_{\text{ad}}$  to  $\text{Br}_{\text{b}}$  atom in the C–Cu–Br–Cu–C bond, indicating that Br atom attracts the majority of electrons from Cu

donation and the electron donation from Cu to C is suppressed. Therefore, the BE of C[C<sub>2</sub>CuBr] is close to that of C[C<sub>3</sub>] (Figure 3). Furthermore, the electron localization function (ELF) mapping demonstrates that the charge is distributed near C<sub>b</sub> and Br<sub>b</sub>, confirming both C–Cu and Cu–Br bonds are ionically bonded (Figure S16b).

In addition, the charge density difference plot shows the evident electron donation from substrate Cu atoms (Cu<sub>sub</sub>) to N atoms, and 0.94 e is transferred from Cu<sub>ad</sub> to N atoms according to Bader charge analysis, further suggesting the strong interaction between N atom and the substrate.

## References

- 1 I. Horcas, R. Fernández, J. M. Gómez-Rodríguez, J. Colchero, J. Gómez-Herrero and A. M. Baro, *Rev. Sci. Instrum.*, 2007, **78**, 013705.
- 2 T. Qin, D. Guo, J. Xiong, X. Li, L. Hu, W. Yang, Z. Chen, Y. Wu, H. Ding, J. Hu, Q. Xu, T. Wang and J. Zhu, *Angew. Chem. Int. Ed.*, 2023, **62**, e202306368.
- 3 G. Kresse and J. Furthmüller, *Phys. Rev. B*, 1996, **54**, 11169-11186.
- 4 G. Kresse and J. Hafner, *Phys. Rev. B*, 1993, **48**, 13115-13118.
- 5 P. E. Blöchl, *Phys. Rev. B*, 1994, **50**, 17953-17979.
- 6 G. Kresse and D. Joubert, *Phys. Rev. B*, 1999, **59**, 1758-1775.
- 7 J. P. Perdew, K. Burke and M. Ernzerhof, *Phys. Rev. Lett.*, 1996, **77**, 3865-3868.
- 8 S. Grimme, *J. Comput. Chem.*, 2006, **27**, 1787-1799.
- 9 J. Tersoff and D. R. Hamann, *Phys. Rev. B*, 1985, **31**, 805-813.
- 10 J. Björk, *J. Phys.: Condens. Matter*, 2016, **28**, 083002.
- 11 G. Henkelman, B. P. Uberuaga and H. Jónsson, *J. Chem. Phys.*, 2000, **113**, 9901-9904.